ELSEVIER

Geoderma 69 (1996) 85–103

GEODERMA

Splash and wash dynamics: An experimental investigation using an Oxisol

R.A. Sutherland [a], Y. Wan [b], A.D. Ziegler [a], C.-T. Lee [a], S.A. El-Swaify [b]

[a] *Geomorphology Laboratory, Department of Geography, University of Hawaii, 2424 Maile Way, Honolulu, HI 96822, USA*

[b] *Department of Agronomy and Soil Science, University of Hawaii, 104 Sherman Laboratory, Honolulu, HI 9682, USA*

Received 15 August 1994; accepted 18 August 1995

Abstract

Limited data are available in the literature on the partitioning of interrill erosion into splash and wash components. Laboratory rainfall simulation experiments were conducted on an Oxisol at 5, 10 and 20° slopes at a constant rainfall intensity. Rainwash was separated from front splash and lateral splash using a novel experimental design. Results indicate that output of sediment from the 0.18 m^2 erosion plots was dominated by splash with a geometric mean aggregate diameter (GMAD) similar to that of the original soil. The most easily detached aggregate size by splash was 500 to 1000 μm, i.e., coarse sand-sized aggregates. Wash was dominated by aggregates with a GMAD significantly finer than the soil matrix, and this reflected the limited energy available to transport coarse aggregates detached by splash. Wash and splash sediment flux, and the runoff coefficient increased significantly with slope angle. Peak front splash was associated with a different dimensionless water depth (DWD) for each slope angle. As slope angle increased the DWD at peak output increased from 0 to 0.4 at 5°, and from 1.4 to 1.7 at 20°. Time trends of front splash output for 5 and 10° slopes were similar to those presented in the literature. However, data for the 20° slopes were more complicated, with a series of pulses related to periodic migrating waves of wash sediment superimposed on the general pattern. These migrating bedload waves are interesting in that they seem analogous to those documented in the fluvial environment at steady or even decreasing discharge. Data indicate that front splash flux exceeded wash transport on all slopes tested. These data reflect the boundary conditions of the experiment, but may be applicable under certain field situations, such as on short, steep, furrow side-slopes.

1. Introduction

Raindrop splash is a phenomenon of interest in atmospheric science, fluid mechanics, soil erosion and in plant disease epidemiology (Yang and Madden, 1993). Since the early

SSDI 0016-7061(95)00053-4

seminal works of Ellison in the 1940s (Ellison, 1944, 1945) there have been numerous contributions to our understanding of rainsplash dynamics, particularly from controlled laboratory investigations (Bryan, 1974; Poesen, 1981; Moss, 1991a, b). Many such studies have focused on disturbed agricultural soils, or more commonly on sediments with limited or no aggregation. These and other fundamental process studies have indicated that splash is a time dependent process, and its importance to soil detachment and transport depends on the following: (1) rainfall characteristics, notably kinetic energy (Bubenzer and Jones, 1971); (2) antecedent moisture status (Al-Durrah and Bradford, 1981); (3) bulk density (Sharma and Gupta, 1989); (4) soil shear strength (Slattery and Bryan, 1992); (5) surface water layer depth (Palmer, 1964); (6) slope angle (Bryan, 1979); (7) surface seal and crust dynamics (Moore and Singer, 1990); and (8) aggregation and stability (Farmer, 1973).

Despite the numerous interrill splash studies there is a significant lack of studies that partition interrill erosion into its sub-components, i.e., splash and wash (interrill overland flow). Separation and quantification of their importance can generally only be achieved in the laboratory, and even this at times has proven problematic. This dearth of detailed sub-process information inhibits the technology transfer of erosion models, such as WEPP. Thus, four objectives were identified for further investigation. These include: (a) the partitioning of interrill sediment output into splash (airsplash) and wash (includes material detached by raindrops and subsequently transported by rain-flow transport processes or overland flow) components; (b) characterization of the temporal dynamics of splash and wash mass aggregate size; (c) quantification of the influence of slope angle on interrill sediment flux, aggregate size and runoff dynamics; and (d) assessment of the influence of a dynamic water layer on splash detachment and transport. These areas of investigation were selected based on inadequate treatment or contradictory results in the soil literature, and a need to incorporate detailed sub-process information from a wider range of soils into state-of-the-art erosion models.

2. Materials and methods

2.1. Soil selection, preparation and characteristics

The Wahiawa Oxisol, a Rhodic Eutrostox, was collected from the Poamoho Experimental Station, central Oahu, Hawaii. The soil was selected for detailed study since there is only limited information on the erosion process dynamics associated with this soil (Dangler and El-Swaify, 1976). It is widely used for pineapple and to a lesser extent, sugarcane production. Erosion of this soil has been linked to nonpoint source pollution, and the physical and chemical characteristics of this soil are well documented (Table 1).

The Wahiawa soil is generally well aggregated and well drained (El-Swaify, 1980); however, under high rainfall intensities this soil is subject to significant erosion (El-Swaify and Cooley, 1980). The soil used in this study was collected from the 0–10 cm depth increment. Samples were air dried, and sieved through a 4-mm square-hole sieve.

Table 1
Characteristics of the Wahiawa Oxisol

Characteristic	Dimensions	Soil depth (cm)	Value(s)
pH in water (1:1)	–	0–10	5.91
Organic carbon	g kg^{-1}	0–10	18.1
CEC	cmol(+)kg^{-1}	0–10	20.8[a]
SiO_2	%	0–10	38.1[b]
Al_2O_3	%	0–10	35.4[b]
Fe_2O_3	%	0–10	18.2[b]
Kaolinite	%	0–10	51.0[c]
Illite	%	0–10	31.0[c]
Amorphous	%	0–10	11.0[c]
Gibbsite	%	0–10	7.9[c]
Hematite	%	0–10	6.2[c]
Particle density	Mg m^{-3}	0–10	2.84
Field bulk density	Mg m^{-3}	0–10	0.97–1.10
Surface area	m^2 g^{-1}	0–10	84.2[d]
Sand (>63 μm)	g kg^{-1}	0–15	40[e]
Silt (2–63 μm)	g kg^{-1}	0–15	160[e]
Clay (<2 μm)	g kg^{-1}	0–15	800[e]
Liquid limit	%	0–10	53.0[f]
Plastic limit	%	0–10	29.0[f]
Activity	–	0–10	0.30[g]
Water retention at saturation	g kg^{-1}	50–75	570[h]
Water retention at 33 kPa	g kg^{-1}	0–15	343[i]
Water retention at 1500 kPa	g kg^{-1}	0–15	246[i]

[a]El-Swaify (1980).
[b]J. Jackman, pers. commun. (1994). X-ray fluorescence.
[c]J. Jackman, pers. commun. (1994). Rietveld refinement of X-ray diffraction: percent of clay fraction except amorphous which is percent of entire soil.
[d]J. Jackman, pers. commun. (1994). glycerol adsorption method.
[e]Determined using the hydrometer method following sonification and chemical dispersion.
[f]Determined using Swedish drop-cone penetrometer.
[g]Activity = (Liquid Limit − Plastic Limit)/Clay %.
[h]Sharma and Uehara (1969).
[i]Thorne (1949).

2.2. Rainfall simulation

A laboratory drip-type simulator based on the design of Munn and Huntington (1976) and described in detail by Garnier (1988) was used in this study. Raindrop fall height was 2.2 m, and uniform drops with a median diameter of 3.2 mm were produced. Domestic water supply with a mean temperature of 21.8 ± 0.8°C (± 1 standard deviation) was used for all tests. Three hour events with an average rainfall intensity of 102 ± 9.0 mm h^{-1} were simulated in this study. High intensity events were used since kinetic energy of rainfall from the simulator was less than natural rainfall (approximately 72%). Additionally, long duration events allowed for the detailed examination of temporal patterns of splash and wash from this well-aggregated soil.

The soil tray used in this study had dimensions of 0.30 m (W) × 0.60 m (L) × 0.10 m (D). The bottom of the tray was covered with a 3-cm layer of glass beads. A metal screen with an attached layer of cheesecloth separated the glass beads from a 7-cm layer of sieved air-dry soil. Soil was gently packed to a mean bulk density of 1.02 ± 0.03 Mg m^{-3}, similar to those found in the field (Table 1). Drainage from the tray was achieved without suction through a drainage outlet at the base of the tray.

2.3. Data collection

Two rainfall events were conducted on slopes of 5, 10 and 20°, and average values are presented for each slope angle in this study. The soil tray was specially fit with two easily detachable lateral splash collectors 0.10 m (W) × 0.60 m (L) × 0.50 m (D), and one detachable front splash collector set 5 mm above the soil surface at the plot outlet. The soil surface was approximately 5 mm below the lip of the lateral splash collectors so that there was no possibility of washover into these collectors. It must be remembered that in the natural situation lateral splash redistribution is not a loss but would be balanced by an input from the surrounding soil. Thus, in laboratory studies there is an artificial decrease in the material redistributed within the plot and this decreases the availability of sediment for wash transport and front splash transport. This may be significant for soils with a limited sediment availability.

Wash was conducted beneath the front splash collector and was funneled to a beaker system. This allowed the sediment output from the erosion tray to be partitioned into that transported from the plot by airsplash and that transported from the plot by a combination of overland flow and rain-flow mechanisms (cf. Moss and Green, 1983), and this latter component will be referred to as wash in this study. Lateral side splash, front splash, and wash samples were collected at 10 min intervals throughout the run. Splash from the upslope end of the plot was collected at the end of each run from the surrounding 0.8 m^3 collector box that housed the soil tray, splash collectors and slope adjustment system. Runoff and percolation volumes were also measured at 10 min intervals. Measurement of runoff was used to determine the runoff coefficient, and this is defined as: [volume of runoff/volume of rainfall] × 100. During each rainfall event periodic plot observations were made. Additionally, times to surface water ponding, runoff initiation and the on-set of percolation were recorded.

Immediately after each run surface bulk density and moisture samples were collected at three to five locations within the plot. A circular ring with an internal diameter of 5.3 cm and a length of 3.0 cm was used. Mass determinations were made prior to and after oven-drying at 105°C for a minimum of 24 h. The soil was removed following the event and replaced with new air-dried, sieved material.

Runoff depths were not directly measured during the event. Instead they were calculated from runoff volumes for each 10-min interval by dividing by the entire contributing area of the plot corrected for slope angle. This assumes equal depth over the entire plot for the 10-min period. As time progressed during the events micro-topographic concentrations and water depth build-up behind micro-dams occurred, but these could not be accounted for using this procedure. However, this approach provides a first approximation to the influence of runoff depth on splash detachment and transport, and wash transport. In this study

Table 2
Variation in time to runoff, final infiltration rate and runoff coefficient with slope angle

Slope (deg)	Time to runoff (min)	Final infiltration rate (mm h^{-1})	Runoff coefficient (%)
5	27.7	63.0	26.3
10	25.5	77.0	16.7
20	17.5	54.0	35.0

dimensionless water depth (DWD) was determined by dividing calculated runoff depth by median drop diameter.

2.4. Aggregate analysis

Following initial sieving of soil through a 4-mm screen a riffle-splitter was used to randomly select five representative samples. These samples were wet-sieved using a procedure similar to that discussed by Gabriels and Moldenhauer (1978). Seven aggregate size fractions were separated in this study, 2000–4000 μm, 1000–2000 μm, 500–1000 μm, 250–500 μm, 125–250 μm, 63–125 μm, and <63 μm.

Immediately after a simulated rainfall event each splash and wash sample was wet-sieved and the seven aggregate size fractions were separated. Total aggregate mass for each 10-min interval was determined by summing the individual aggregate size fractions. For fractions coarser than 63 μm material was placed in small pre-weighed 50-ml aluminum tins, decanted and oven-dried for 24 h at 105°C. Mass of each aggregate fraction was determined to a precision of ± 0.001 g. Dilute nitric acid was added to the suspension passing the 63 μm screen and this was left to settle for 36–48 h then decanted and oven-dried in 250-ml beakers.

Geometric mean diameters for the wet-sieved splash and wash aggregates were determined for the Wahiawa soil using the equation of Kemper and Rosenau (1986):

$$\mathrm{GMAD} = \exp\left(\frac{\sum_{i=1}^{n} w_i \log \bar{X}_i}{\sum_{i=1}^{n} w_i}\right) \quad (1)$$

where GMAD is the geometric mean aggregate diameter (mm), w_i is the mass (g) of an individual size fraction, $\bar{X}_i$ is the mean sieve size, and $\sum_{i=1}^{n} w_i$ represents the total sample mass.

3. Results and discussion

3.1. Runoff and infiltration

Time to runoff generation decreased with increasing slope angle from 27.7 min for the 5° slope to 17.5 min for the 20° slope (Table 2). Infiltration rates decayed from 102

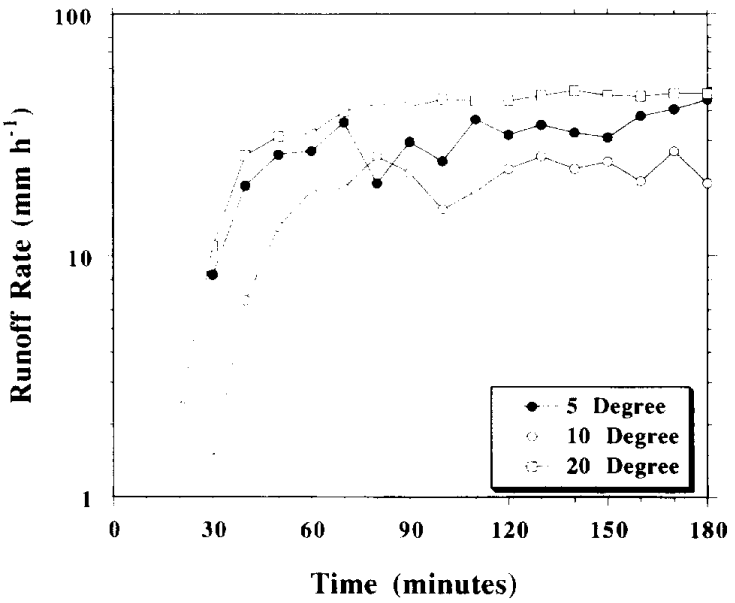

Fig. 1. Temporal relationship of runoff rate from an Oxisol for three slope angles. Each curve represents the average of two replicates.

mm h^{-1} to approximately 54 mm h^{-1} for the 20° slope (after 3 h). The 20° slope produced 2.1 times the runoff volume of the 10° slope, and the time integrated runoff coefficient was 35%. The temporal variation in runoff rate (Fig. 1) indicates similar patterns for all slopes, with runoff more variable from the 5 and 10° slopes. A steady-state condition was reached after about 70 min for the 20° slope. Observations indicated that some of the variability in the 5 and 10° slopes was attributed to the development of micro-dams which would periodically overtop or disintegrate through erosion therefore releasing pulses of water.

Poesen (1987) noted contradictory results from the literature dealing with the relationship between slope angle and infiltration or runoff. His field and laboratory results indicated a decrease in infiltration rate with increasing slope angle on soils that were prone to surface sealing, soil textures examined ranged from fine sand to silts. Poesen's results differed from those in this study, which showed a more complicated response with slope angle (Table 2), and the infiltration rates followed the sequence: $10° > 5° > 20°$. Some of this variability may be attributed to the variation in erosion dynamics associated with surface seal development. Another possible reason may be the variation in median aggregate size of the surface soil as suggested by Luk (1983).

3.2. *Runoff depth and front splash*

Little is known about the influence of a moving water layer on splash output from plots, fields, or to rills, with increasing slope angle. The reason for this is that it is difficult to measure in the field, and few laboratory studies have effectively partitioned these components.

Different relationships exist between front splash and calculated DWD for the three slope angles (Fig. 2). Data were smoothed using robust locally weighted regression estimates, lowess (Cleveland and Devlin, 1988). Maximum front splash for the 5° slope was associated with DWD values of 0 (near saturation) to about 0.4. As slope angle increased the water

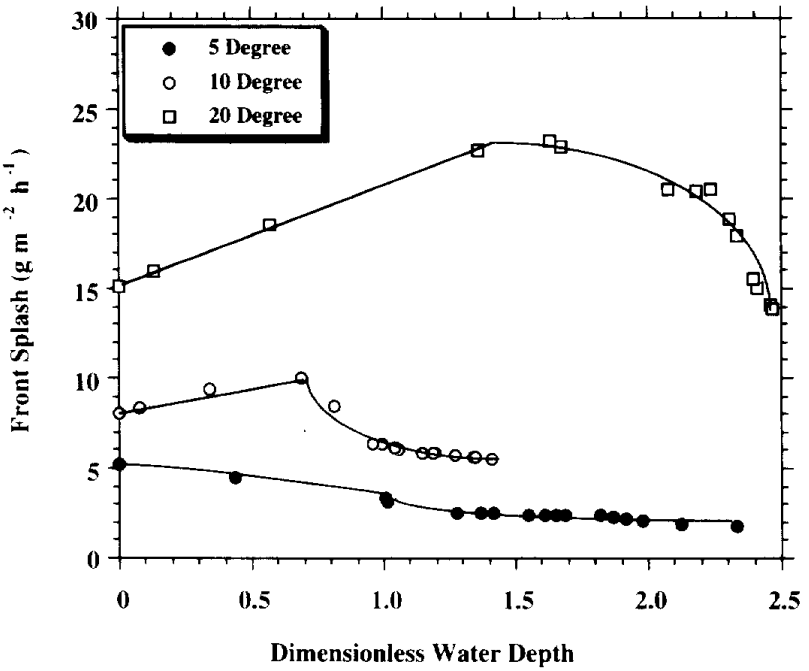

Fig. 2. Relationship of calculated dimensionless water depth and front splash transport. Each curve represents the average of two replicates.

depth at peak splash increased from a DWD of 0.7 at 10° to a DWD of 1.4–1.7 for the 20° slope. The present DWD values fall within those given in the literature for peak rainsplash (Table 3). However, it is important to note that many of these studies have used only small splash containers, on gentle slopes ($< 1°$), with a static water layer. It was not until the experimental work of Moss and Green (1983), on quartz sand, that the importance of a dynamic water layer on airsplash was observed.

These results have significant implications for modeling soil detachment. Presently available soil erosion models such as EUROSEM (Morgan et al., 1992) and SHE (Wicks et al., 1992) include depth of a surface layer in their algorithms for soil detachment prediction. EUROSEM includes the factor $\exp(-bh)$, where b is an exponent that is a function of soil texture, and h is the depth of the surface water layer (which assumes detachment by raindrop impact decreases as water depth increases). SHE includes a more complex F_w parameter, where $F_w = 1$ if water depth (h) is less than or equal to the median drop diameter (d_{50}), and if $h > d_{50}$ the equation becomes $F_w = \exp(1 - h/d_{50})$. Results from the present study indicate that both of these equations are oversimplifications for steep slopes with time varying surface conditions. The algorithm for interrill detachment rate in the WEPP model (Elliot et al., 1989), which is also incorporated into PRORIL (Lewis et al., 1994), has no separate parameterization for surface water depth.

3.3. Splash detachment and transportation

Cumulative front splash material varied significantly with slope angle (Fig. 3). The mass ratio of airsplashed material increased in the following sequence, 1.0:2.5:6.8 for 5, 10 and 20° slopes. The relationship between slope angle and splash has been addressed in the literature, but no consistent relationship has been observed. This is based partly on the

Table 3
Literature summary of the relationship between peak splash and dimensionless water depth

Reference source[a]	Slope (deg)	Splash apparatus	Material	RFI[b] (mm h^{-1})	Water layer	DD[c] (mm)	Dimensionless water depth
1	0	5.4-mm container	Soil (7% sand, 55% silt)	–	Static	2.9	0.69
1	0	5.4-mm container	Soil (7% sand, 55% silt)	–	Static	4.7	0.85
1	0	5.4-mm container	Soil (7% sand, 55% silt)	–	Static	5.9	1.02
2	0	Thin-walled rectangular tray (no dimensions)	Quartz sediment, $D_{50}=0.24$ mm, $D_{90}=0.92$ mm	100	Static	2.7	0 to 0.19
3	< 0.3	50 × 50 cm tray	Quartz, $D_{50}=0.20$ mm	64	Dynamic	1.27	1.8
3	< 0.3	50 × 50 cm tray	Quartz, $D_{50}=0.20$ mm	64	Dynamic	2.70	0.8
3	< 0.3	50 × 50 cm tray	Quartz, $D_{50}=0.20$ mm	64	Dynamic	5.10	0.5
4	0	10.2-cm container	Soil, silt loam	102	Static	1.6	Near saturation
5	0	5-cm diameter petri dish	Various	–	Static	3.0–6.2	Near saturation
6	–	2.0 m × 0.5 m tray	Soil, 3 clays and 1 sandy loam	15–60	Static	–	Near saturation
7	< 0.6	5.8 m × 1.0 m flume	Vertisol (16.3% sand, 21.5% silt)	40	Dynamic	2.24	0.89 > 2.23 > 4.46
7	< 0.6	5.8 m × 1.0 m flume	Aridisol (46.6% sand, 21.2% silt)	40	Dynamic	2.24	0.89 > 2.23 > 4.46

[a] 1 = Palmer (1964); 2 = Moss et al. (1979); 3 = Moss and Green (1983); 4 = Schultz et al. (1985); 5 = Ghadiri and Payne (1986); 6 = Torri et al. (1987); 7 = Proffitt and Rose (1991).
[b] RFI = rainfall intensity.
[c] DD = drop diameter.

different experimental designs used in the field or in the laboratory. Examination of the front splash flux in this study is analogous to the output from the downslope segment of a hillslope with no, or limited, compensatory upslope movement. This can be envisioned as

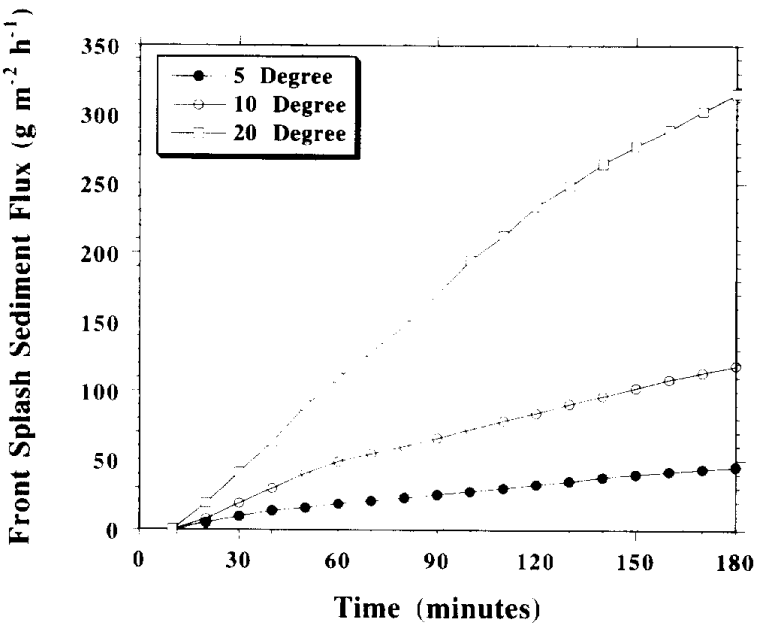

Fig. 3. Cumulative front splash sediment transport for three slope angles. Each curve represents the average of two replicates.

transport to a rill, furrow, gully or stream network from short, steep slopes. Under these boundary conditions we found splash output increased significantly ($P=0.05$) with slope angle from 5 to 20°.

The time-trends of front splash output (Fig. 4) for 5 and 10° slopes are very similar. For all slopes splash was low during the initial 10-min period. Peak splash for the 5° slope occurred between the 10–20 and 30–40 min time periods. For the 10° slope the peak was delayed and occurred between 20–30 and 40–50 min time periods. Following peak splash,

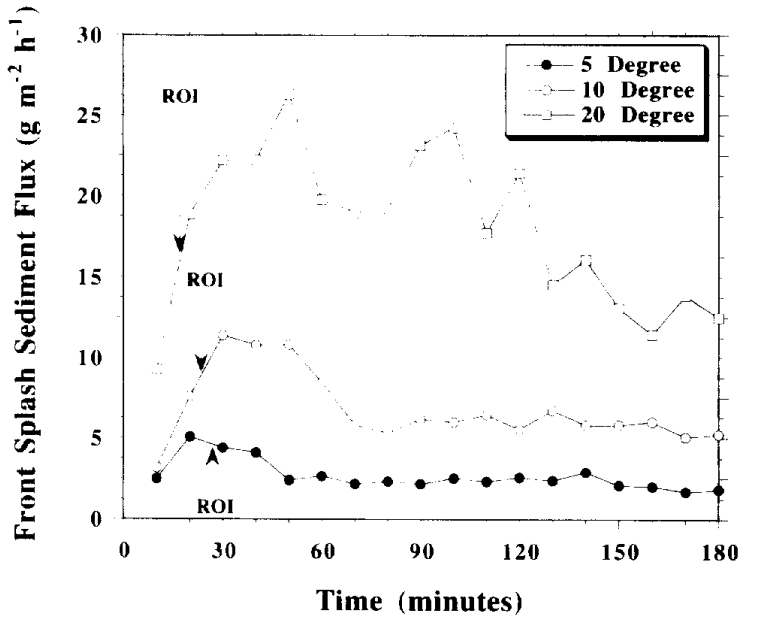

Fig. 4. Temporal variation in front splash sediment flux for three slope angles. Note ROI represents time of runoff initiation.

output decayed to a steady-state condition for both 5 and 10° slopes. This pattern is similar to the three-stage model discussed by Chen et al. (1980) and Moore and Singer (1990). The pattern for the 20° slope was more complicated, indicating several periods of high splash transport 40–50 min, 80–100 min, and 110–120 min before decreasing, but no steady-state condition was reached after 3 h. These pulses were related to areas of water concentration and micro-topographic undulations. Observations indicated that these forms were transient in nature and produced small-scale colluvial fans which acted like micro-dams. Once over topped or eroded this sediment was flushed downslope. No headcutting or micro-rill bank failure was observed. Periods of increased splash were associated with increased periods of wash transport, where pulses of flow-driven sediment were output from the plot. These wash pulses may be considered analogous to bedload pulses noted in fluvial systems under steady discharge conditions or even during decreasing discharge periods (Reid and Frostick, 1987; Gomez, 1991). During the 20° simulations, as pulses of sediment moved downslope towards the outlet of the erosion tray, the availability of material for airsplash was increased and thus there was a concomitant increase in splash.

The general temporal patterns of airsplash for the 5 and 10° slopes were very similar to those described in the literature despite very different scales of measurement, different techniques and types of apparatus used for collection, both static and dynamic water layers were considered, and the similarity between results for primary particles (soil H of Poesen, 1981) and well-aggregated clay (Heiden, air-dry soil, Truman and Bradford, 1990). Thus, similarity in temporal airsplash patterns between such diverse materials is suggestive of fundamental underlying processes operating at the soil surface for slopes $\leq 10°$.

The following phases can generally be identified in temporal patterns of splash: (1) On initially air-dry soil impacting raindrops and the generation of lateral jets can cause macro-aggregate breakdown by slaking or shearing off micro-aggregates or primary particles. Moore and Singer (1990) suggests that this early phase is characterized by an energy-limited transport capacity. (2) With increasing moisture content and the development of a thin water layer rainflow transport increases (Moss, 1988), and this is associated with the reduction of surface soil strength, and maximum breakdown of structural units occurs (Farres, 1987). (3) Partial surface seals develop by various mechanisms including compaction, skin seal formation, filtration pavements, chemical dispersion, and with time they increase the surface's resistance to lateral shear and normal raindrop impact forces. The combination of increased soil strength and exceedance of a threshold water depth causes splash to decrease. (4) Significant areas of the surface may be covered by a seal, this combined with limited particle availability produces a steady-state splash condition. Absence of a steady-state splash condition, especially on steep slopes, may reflect seal breakdown by the shear stress of overland flow, or as in this study it may reflect the downslope pulse of material by overland flow that becomes available for splash transport. The four-phase model discussed above seems to fit the data from the literature and that presented in this study.

It should be noted that not all soils are subject to significant seal development. El-Swaify (1980) states, certain Oxisols, when bare, display surface sealing due to raindrop impact. Limited bulk density data from this study indicate that compaction of the surface occurred, with increases less than 10% on all slopes after a 3-h event. These bulk density values represent increases averaged over a depth of 3 cm. Thus, given that the thickness of skin

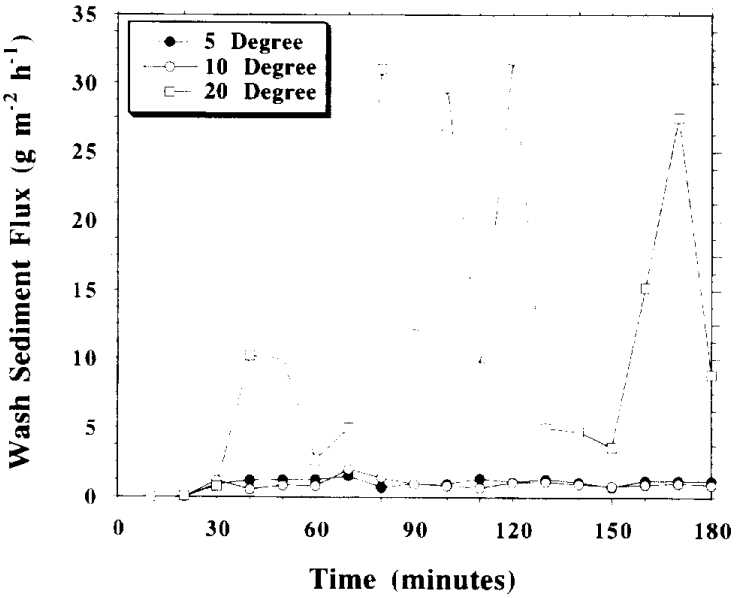

Fig. 5. Temporal variation in wash sediment flux for three slope angles. Each curve represents the average of two replicates.

layer seals for temperate soils are ≤ 0.12 mm and densified sub-layers range in thickness from 0.002 to 0.33 mm (Remley and Bradford, 1989) it is likely that seal layer densities for the Wahiawa soil increased to a much greater extent than the presently available data indicate. In fact, data from a separate study on the Wahiawa Oxisol indicated that sampling a thin 5-mm surface layer after rainfall simulation (100 mm h^{-1}, 3-h duration) produced increases in bulk density of 40–50% (C.-T Lee, pers. commun., 1994).

3.4. Wash detachment and transport

Wash transport from the 5 and 10° slopes did not differ significantly at $P=0.05$ using the nonparametric Wilcoxon signed rank test. Cumulative output for the 5 and 10° slopes was about 17.2 g m^{-2} h^{-1} (0.17 Mg ha^{-1} h^{-1}), or 12 times lower than that for the 20°slope (2.1 Mg ha^{-1} h^{-1}). Sediment pulses were only observed for the 20° slope treatments (Fig. 5). The earliest pulse occurred at 30–50 min, and more significant ones were recorded at 70–80, 90–100, 110–120 and 160–170 min. Several of these are directly linked with the increased airsplash noted earlier. Pulses were unrelated to fluctuations in runoff rate, since runoff for the 20° slope reached an approximate steady-state at 70 min (Fig. 1). Pulses reflect the internal plot storage dynamics, and the downslope movement of material on short slope lengths, similar to agricultural furrows. It is difficult to envision the adequate modeling of such pulses within the presently available soil erosion interrill models. In the WEPP interrill model erodibility (K_i) is defined at steady-state runoff and steady-state sediment flux on small bounded plots (0.375 m^2; cf. Elliot et al., 1989). However, results from the 20° experiments indicate an extremely wide range in K_i values would be obtained over very short time periods despite steady-state flow conditions. The calculated K_i value at 110–120 min was 2.59×10^6 kg s m^{-4} (during a wash pulse and front splash peak) and only 9.52×10^5 kg s m^{-4}, or 2.7 times, less during the subsequent time period, i.e., 120–130 min

Table 4
Comparison of splash and wash ratios for the Wahiawa Oxisol to those for different soil textures

Reference source	RFI (mm h^{-1})	Duration (h)	Slope (deg)	Texture	Splash: Wash ratio
Bryan (1974)[a]	102	1.5[b]	20	Clay	1:1.87[c]
Bryan (1974)	102	1.5	20	Sandy clay loam	1:2.02[c]
Bryan (1974)	102	1.5	20	Clay loam	1:1.91[c]
Bryan (1974)	102	1.5	20	Loam	1:1.56[c]
Bryan (1974)	102	1.5	20	Sandy loam	1:2.48[c]
Bryan (1974)	102	1.5	20	Silt loam	1:1.41[c]
Bryan (1974)	102	1.5	20	Loamy sand	1:1.90[c]
Luk (1979)[d]	102	0.5	3–30	Loam to sandy loam	3.74:1[c]
This study	102	3.0	5	Clay	26.23:1[c]
This study	102	3.0	10	Clay	38.75:1[c]
This study	102	3.0	20	Clay	4.81:1[c]
Bryan and Luk (1981)[e]	68.6	1.0	12.5	Silty clay loam	1:12.66[f]
Bryan and Luk (1981)	61.6	1.0	12.5	Sandy loam	1:22.45[f]
Bryan and Luk (1981)	63.7	1.0	12.5	Silt loam	1:4.86[f]
This study	102	3.0	5	Clay	2.63:1[f]
This study	102	3.0	10	Clay	7.51:1[f]
This study	102	3.0	20	Clay	1.56:1[f]

[a]Edmonton-type spray simulator with a median drop diameter of 1.1 mm and a fall height of 2.49 m, soil presieved through a 6.19-mm square-hole sieve.
[b]Based on the following sequence: air-dried soils subjected to 30 min of rainfall, a 60 min drying period, a further 30 min of rainfall, 15 min drying, and a final 30 min rainfall.
[c]Represents total splash (front + lateral + top): wash ratio.
[d]Edmonton-type spray simulator, plot area = 0.093 m^2, soil was presieved using a 4-mm square-hole sieve, and bulk densities of 0.71 to 0.99 Mg m^{-3} were used.
[e]Edmonton-type spray simulator, soil presieved through a 8-mm square-hole sieve, and soils were pre-wet.
[f]Represents front splash: wash ratio.

(a non-pulse period). To our knowledge similar pulses in the soil erosion literature have not been documented.

3.5. *Splash and wash comparisons*

Several laboratory studies have attempted to separate the magnitude of splash and wash contributions to soil erosion. However, in some cases the experimental set-up prevented the effective partitioning of wash from splash at the plot outlet. The studies by Bryan (1974) and Luk (1979) partitioned total splash (lateral + front + top) from wash output, and the study of Bryan and Luk (1981) partitioned front splash and wash from a plot outlet. Data from these studies are compared with those from the present investigation (Table 4). It is recognized that it is difficult to make direct comparisons of erosion results from different simulators even when the same soil is used (Bryan and De Ploey, 1983). However, the magnitude of differences between the results from Bryan (1974) and Bryan and Luk (1981) and those from this study for total splash or front splash are very large. Their data were obtained from experiments conducted on a variety of soil textures and indicate that splash $\ll$ wash. Data from the present study (clay-rich Oxisol) indicate the exact opposite

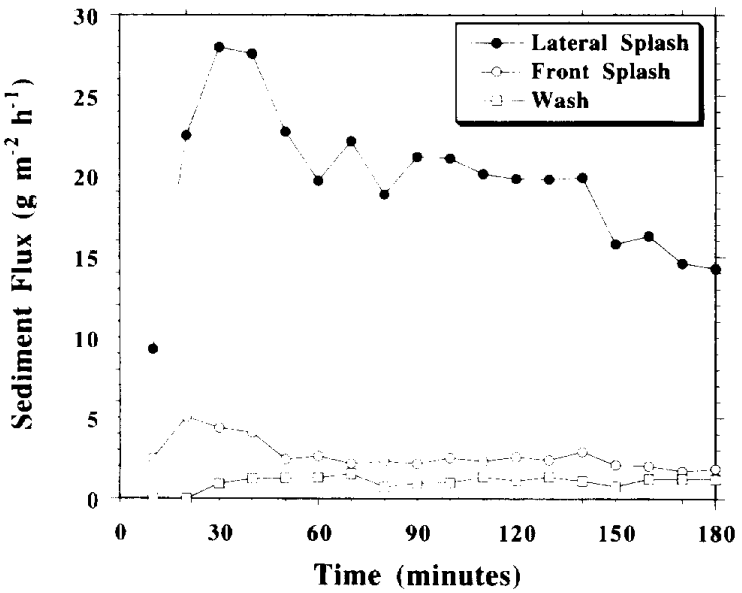

Fig. 6. Temporal variation in lateral (side) splash redistribution, front splash and wash for the 5° slope. Each curve represents the average of two replicates.

pattern splash ≫ wash. Assuming both studies effectively separated total splash and front splash from wash the different results may reflect differences in rainfall energy, soil preparation, rainfall duration, infiltration rates, runoff energy, aggregate stability, susceptibility of individual soils to crust or seal, and water layer development. The data from Luk (1979) (Table 4) represent mean values for four soils from Canada (one alpine, two grassland, and one cultivated), and three slope angles (3, 10 and 30°). His data indicate total splash > wash, with a ratio of 3.7:1.0 which is similar to that for the 20° slope in the present investigation 4.8:1.0.

The temporal variation in lateral splash, front splash and wash for the 5° slope (Fig. 6) and the 20° slope (Fig. 7) exhibit some interesting patterns. Data for the 10° slope are not shown but are similar to those for the 5° slope. Note that for slopes $\leq 10°$ significantly more material is redistributed by lateral airsplash than output by front splash and wash combined. For the 20° slope significantly more material is output by wash and front splash as compared to the 5 and 10° slopes. At specific times the total output of wash plus front splash exceeds lateral redistribution (Fig. 7), particularly during the pulse event periods. But, for the entire 3-h event lateral redistribution is the greatest component, indicating even on such small plots the sediment delivery ratio is $\ll 100\%$. A one-way analysis of variance followed by a Fisher's protected least significant difference test indicated that lateral splash increased significantly ($P = 0.05$) with slope angle. Median lateral splash values for 36 10-min increments were 18.9 (5° slope) < 25.8 (10° slope) < 36.1 g m^{-2} h^{-1} (20° slope).

A plot of front splash and wash for each time increment ($n = 36$) for all three slopes (Fig. 8) indicates the relative importance of splash to total sediment output given the boundary conditions of the present study. Even if an upslope splash component is considered, front splash exceeded wash. Thus, splash as an interrill transport mechanism may be important under the following conditions: (1) small bounded plots with open surface collectors, limited overland flow generation due to low rainfall intensity, or high infiltration capacity; and (2) short, steep furrow side-slopes, typical of agricultural areas. In the latter

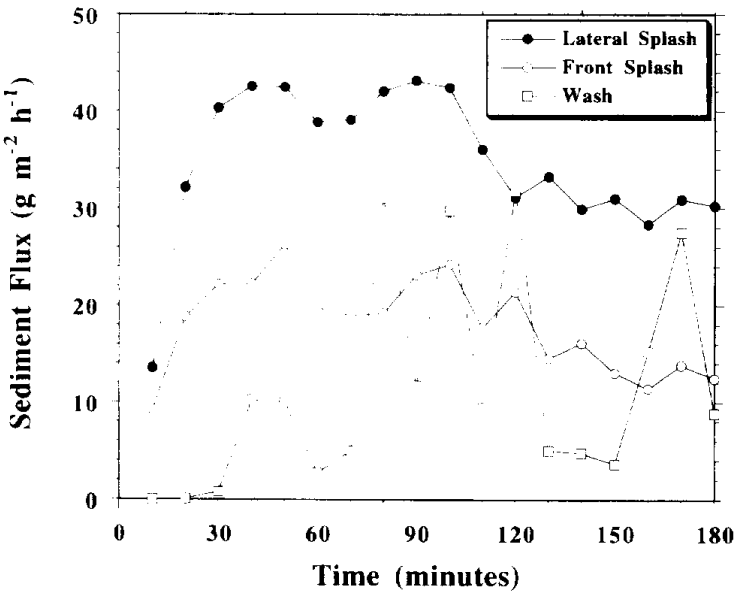

Fig. 7. Temporal variation in lateral (side) splash redistribution, front splash and wash for the 20° slope.

environments direct transport to a flow system would occur with little upslope sediment movement from the furrow to the side-slope. Under natural hillslope conditions wash would be the dominant interrill transport process, but splash near the interface of interrill–rill areas may be more important than previously identified if depths of water accumulation are restricted.

3.6. Geometric mean aggregate diameter

The wet-sieved GMAD of the test soil ranged from 660 to 730 μm (i.e., coarse sand-size aggregates). The median GMAD values for wash and front splash for each of the three slopes are shown graphically in Fig. 9. Aggregates transported by wash consistently had GMAD values in the medium sand-size range, i.e., significantly smaller than the original test soil, by about 300 to 450 μm. Wash GMAD values were significantly larger for the 20° slope due to increased flow competence associated with increased runoff and associated increase in shear stress and stream power. These data support previous work suggesting that interrill overland flow preferentially transports particles finer than the soil matrix (Alberts et al., 1983). On the other hand, splash-transported particles did not significantly differ in size from the original soil matrix. Therefore, the dominance of splash over wash in interrill material collected from steep, short slopes with open troughs (i.e., a non-Gerlach type troughs) may partially account for some studies documenting limited selectivity of interrill transported sediment, e.g., furrow side-slopes (Meyer et al., 1992). The GMAD values for splash did not significantly differ with slope angle, and median values were in the range of coarse sand-sized aggregates. A comparison by means of a box-plot (Fig. 9) indicates no overlap in the 95% confidence bands of the median GMAD between wash and splash. This indicates that splash is statistically coarser than wash, but not different from the original soil.

In this study splash had the ability to detach a range of particles from <63 μm to 2000–4000 μm, however runoff was not energetic enough to move the coarser particles. The

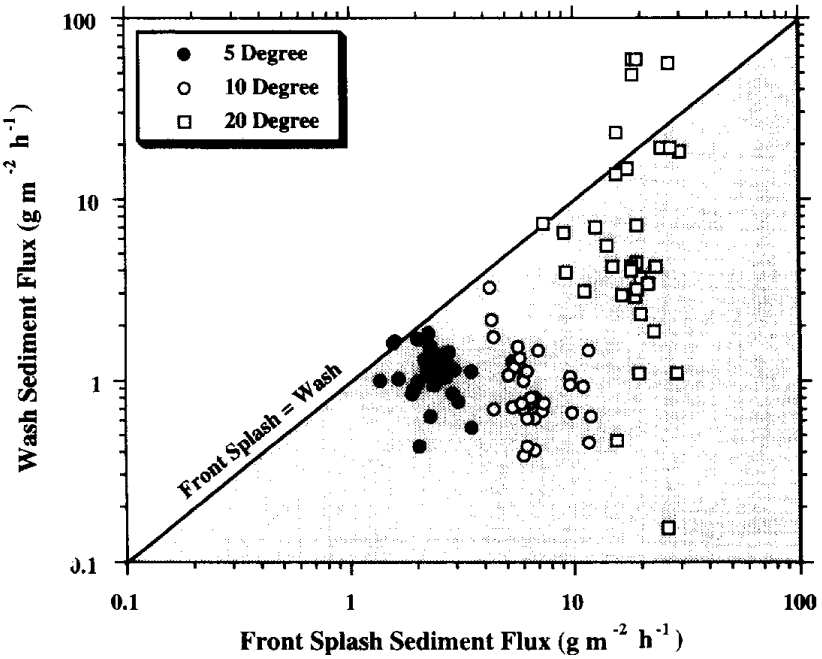

Fig. 8. Relationship between wash sediment flux and front splash sediment flux. Each curve represents the average of two replicates.

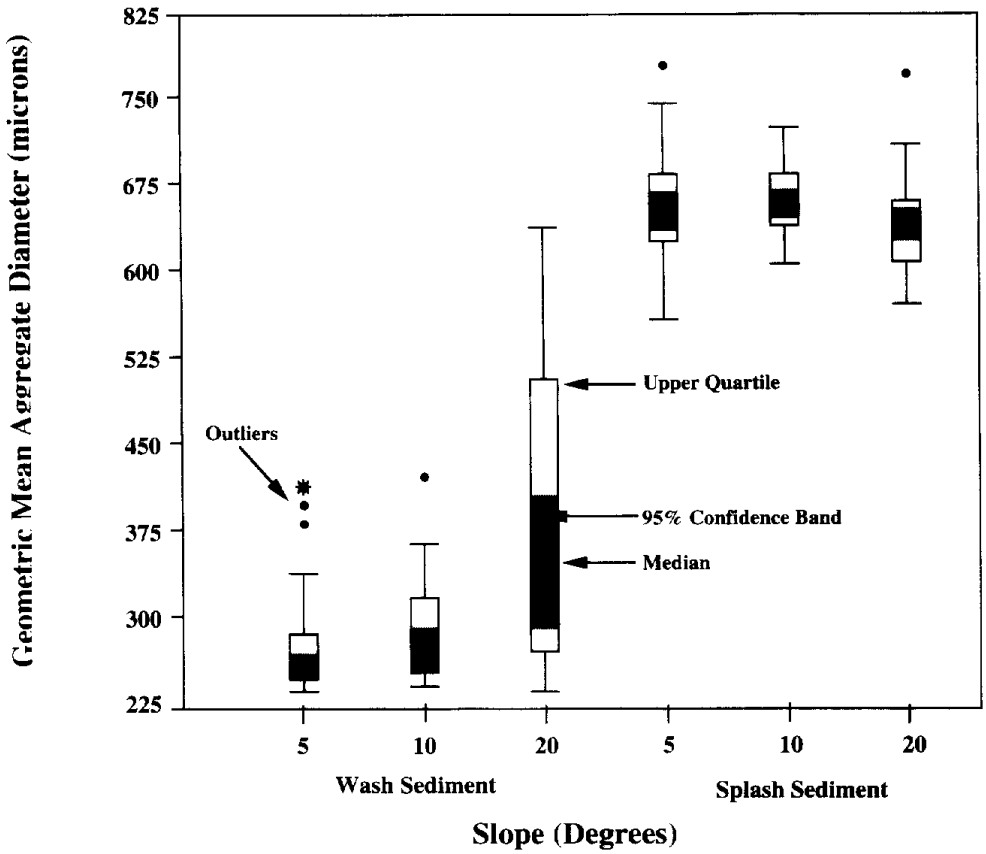

Fig. 9. Box-plot of geometric mean aggregate diameter (GMAD) for wash and splash sediment and their relationship with slope angle.

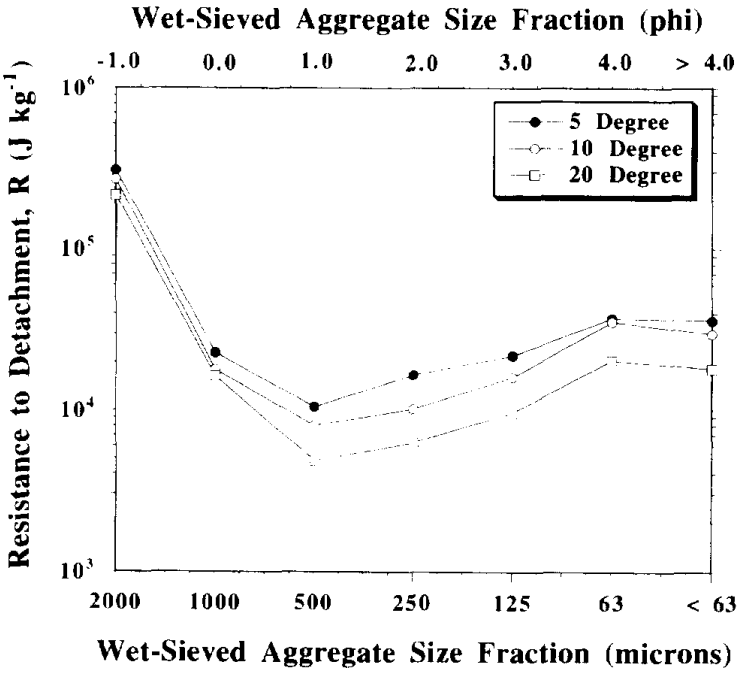

Fig. 10. Resistance of individual aggregate size fractions to splash detachment and the influence of slope angle. Note that 2000 implies a size range of 2000–4000 μm; 1000, 1000–2000 μm; 500, 500–1000 μm; 250, 250–500 μm; 125, 125–250 μm; 63, 63–125 μm.

coarser particles were deposited and redetached by raindrop impact. Even though rainfall impact has a greater energy flux density than runoff not all soil particles are equally detachable by splash. A useful index for a soil is its resistance to detachment (R), and is the energy (J) required to detach 1 kg of soil. This index has been used by De Ploey and Poesen (1985) and Poesen (1985, 1986). The R-value for splash has been exclusively applied to whole soils, here the R-value was defined for each wet-sieved aggregate size fraction. The R-values (Fig. 10) indicate that the most resistant fraction to splash detachment was 2000–4000 μm, while the least resistant fraction was 500–1000 μm. This latter population includes the GMAD of the original soil. Also from Fig. 10 it is apparent that the resistance of individual aggregate size fractions decreases significantly with increasing slope angle, i.e., less energy is required to move 1 kg of a particular aggregate fraction as slope increases (Fig. 10). Decreases in whole-soil R-values with increasing slope angle (1 to 7°) were noted by Savat (cited in Poesen, 1985). Thus, curves similar to Fig. 10 for particular aggregate size fractions may be invaluable for incorporation into future soil erosion models.

4. Conclusions

In this study runoff volume from 20° slopes was 1.6 times that from the 5 and 10° slopes combined. This runoff difference resulted in a 12 times increase in sediment transport by wash for a 3-h rainfall event from the 20° slope treatment. Wash output for the 5 and 10° slopes was not significantly different ($P=0.05$) and their temporal output patterns were similar with no transport rate greater than 3.2 g m^{-2} h^{-1} (0.032 Mg ha^{-1} h^{-1}). The wash data for the 20° slopes indicated a peak transport rate approximately 18 times greater than

that for the gentler slope treatments. The temporal pattern of wash output for the 20° slope was unusual, since it showed a series of aperiodic pulses. These pulses were observed under steady discharge conditions during 20° runs, and represented the slow downslope migration of sediment waves. These pulses may be analogous to those described in the fluvial literature for bedload, which can occur under steady discharge or even under decreasing discharge conditions.

Dimensionless water depth at peak splash transport varied with slope angle, from 0–0.4 at 5° slopes to 1.4–1.7 at 20° slopes. The only other comparable data in the literature are from Moss and Green (1983) and Moss (1988) for non-aggregated material (quartz sediment) at low slope angles ($<0.3°$). Integration of this type of information is required for future developments of physically based erosion models.

Temporal variation in splash for 5 and 10° slopes were similar to those described in the literature for soils and non-aggregated sediments. The temporal relationship for the 20° slope was more complicated since there was an interaction with wash pulses superimposed on the general time sequence identified for the gentler slope treatments.

The ratio of front splash to wash decreased from 26–39: 1 for 5 and 10° slopes to 5:1 for 20° slopes. This pattern reflects increasing shear stress and stream power associated with increased runoff depth and slope angle. However, it is important to emphasize the importance of splash as not only an effective detachment mechanism but also as an important transport mechanism of sediment from the soil tray. These results may also be applicable to short, steep furrow side-slopes commonly found in agricultural areas. With longer slope segments wash processes would dominate the interrill sediment flux.

Acknowledgements

The research was supported by the U.S. Department of Agriculture under Section 406, Food for Peace, Cooperative State Research Service Special Grant Agreement No. 91-34135-6177, managed by the Pacific Basin Administrative Group (PBAG) to R.A. Sutherland and S.A. El-Swaify, and their support is gratefully acknowledged. The assistance of E. Grossman, S. Siddiqui and C. Wilburn in the early phase of this study is also gratefully acknowledged. We are also greatly appreciative of the constructive comments of the three anonymous reviewers of this paper.

References

Alberts, E.E., Wendt, R.C. and Piest, R.F., 1983. Physical and chemical properties of eroded soil aggregates. Trans. Am. Soc. Agric. Eng., 26: 465–471.

Al-Durrah, M. and Bradford, J.M., 1981. New methods of studying soil detachment due to waterdrop impact. Soil Sci. Soc. Am. J., 45: 949–953.

Bryan, R.B., 1974. Water erosion by splash and wash and the erodibility of Albertan soils. Geogr. Ann., 56A: 159–181.

Bryan, R.B., 1979. The influence of slope angle on soil entrainment by sheetwash and rainsplash. Earth Surf. Process., 4: 43–58.

Bryan, R.B. and De Ploey, J., 1983. Comparability of soil erosion measurements with different laboratory rainfall simulators. Catena Suppl., 4: 32–56.

Bryan, R.B. and Luk, S-H., 1981. Laboratory experiments on the variation of soil erosion under simulated rainfall. Geoderma, 26: 245–265.

Bubenzer, G.D. and Jones, B.A., Jr., 1971. Drop size and impact velocity effects on the detachment of soils under simulated rainfall. Trans. Am. Soc. Agric. Eng., 14: 625–628.

Chen, Y., Tarchitzky, T., Brouwer, J., Morin, J. and Banin, A., 1980. Scanning electron microscope observations on soil crusts and their formation. Soil Sci., 130: 49–55.

Cleveland, W.S. and Devlin, S.J., 1988. Locally weighted regression: An approach to regression analysis by local fitting. J. Am. Stat. Assoc., 83: 596–610.

Dangler, E.W. and El-Swaify, S.A., 1976. Erosion of selected Hawaii soils by simulated rainfall. Soil Sci. Soc. Am. J., 40: 769–773.

De Ploey, J. and Poesen, J., 1985. Aggregate stability, runoff generation and interrill erosion. In: K.S. Richards, R.R. Arnett and S. Ellis (Editors), Geomorphology and Soils. George Allen & Unwin, London, pp. 99–120.

Elliot, W.J., Liebenow, A.M., Laflen, J.M. and Kohl, K.D., 1989. A Compendium of Soil Erodibility Data From WEPP Cropland Soil Field Erodibility Experiments 1987 & 1988. NSERL Report No. 3, The Ohio State University and USDA ARS, 317 pp.

Ellison, W.D., 1944. Studies of raindrop erosion. Agric. Eng., 25: 131–136.

Ellison, W.D., 1945. Some effects of raindrops and surface-flow on soil erosion and infiltration. Trans. Am. Geophys. Union, 26: 415–429.

El-Swaify, S.A., 1980. Physical and mechanical properties of Oxisols. In: B.K.G. Theng (Editor), Soils with Variable Charge. New Zealand Soc. of Soil Sci., Offset Publications, Palmerston North, pp. 303–324.

El-Swaify, S.A. and Cooley, K.R., 1980. Sediment Losses from Small Agricultural Watersheds in Hawaii (1972–1977). USDA, Sci. and Education Admin., Agric. Reviews and Manuals, ARM-W-17, 124 pp.

Farmer, E.E., 1973. Relative detachability of soil particles by simulated rainfall. Soil Sci. Soc. Am. Proc., 37: 629–633.

Farres, P.J., 1987. The dynamics of rainsplash erosion and the role of soil aggregate stability. Catena, 14: 119–130.

Gabriels, D. and Moldenhauer, W.C., 1978. Size distribution of eroded material from simulated rainfall: Effect over a range of texture. Soil Sci. Soc. Am. J., 42: 954–958.

Garnier, C.L., 1988. Residue effects on runoff and erosion under simulated rainfall from steeply sloping tropical soils. Ph.D. Thesis, University of Hawaii, Dept. Agronomy and Soil Sci., 400 pp., unpubl.

Ghadiri, H. and Payne, D., 1986. The risk of leaving the soil surface unprotected against falling rain. Soil Tillage Res., 8: 119–130.

Gomez, B., 1991. Bedload transport. Earth-Sci. Rev., 31: 89–132.

Kemper, W.D. and Rosenau, R.C., 1986. Aggregate stability and size distribution. In: A. Klute (Editor), Methods of Soil Analysis, Part 1. Physical and Mineralogical Methods (2nd ed.). Am. Soc. Agronomy and Soil Sci. Soc. Am., Agronomy Monograph No. 9, Madison, WI, pp. 425–442.

Lewis, S.M., Storm, D.E., Barfield, B.J. and Ormsbee, L.E., 1994. PRORIL — An erosion model using probability distributions for rill flow and density II. Model validation. Trans. Am. Soc. Agric. Eng., 37: 125–133.

Luk, S.-H., 1979. Effect of soil properties on erosion by wash and splash. Earth Surf. Process., 4: 241–255.

Luk, S.-H., 1983. Effect of aggregate size and microtopography on rainwash and rainsplash erosion. Z. Geomorphol., 27: 283–295.

Meyer, L.D., Line, D.E. and Harmon, W.C., 1992. Size characteristics of sediment from agricultural soils. J. Soil Water Conserv., 47: 107–111.

Moore, D.C. and Singer, M.J., 1990. Crust formation effects on soil erosion processes. Soil Sci. Soc. Am. J., 54: 1117–1123.

Morgan, R.P.C., Quinton, J.N. and Rickson, R.J., 1992. EUROSEM: Documentation Manual, Version 1. Silsoe College, Bedford, U.K., 34 pp.

Moss, A.J., 1988. Effects of flow-velocity variation on rain-driven transportation and the role of rain impact in the movement of solids. Aust. J. Soil Res., 26: 443–450.

Moss, A.J., 1991a. Rain-impact soil crust. I. Formation on a granite-derived soil. Aust. J. Soil Res., 29: 271–289.

Moss, A.J., 1991b. Rain-impact soil crust. II. Some effects of surface-slope, drop-size and soil variation. Aust. J. Soil Res., 29: 291–309.

Moss, A.J. and Green, P., 1983. Movement of solids in air and water by raindrop impact: Effects of drop-size and water-depth variations. Aust. J. Soil Res., 21: 257–269.

Moss, A.J., Walker, P.H. and Hutka, J., 1979. Raindrop-stimulated transportation in shallow water flows: An experimental study. Sediment. Geol., 22: 165–184.

Munn, J.R., Jr. and Huntington, G.L., 1976. A portable rainfall simulator for erodibility and infiltration measurements on rugged terrain. Soil Sci. Soc. Am. J., 40: 622–624.

Palmer, R.S., 1964. The influence of a thin water layer on waterdrop impact forces. Int. Assoc. Sci. Hydrol. Publ., 65: 141–148.

Poesen, J., 1981. Rainwash experiments on the erodibility of loose sediments. Earth Surf. Process. Landforms, 6: 285–307.

Poesen, J., 1985. An improved splash transport model. Z. Geomorphol., 29: 193–211.

Poesen, J., 1986. Field measurements of splash erosion to validate a splash transport model. Z. Geomorph. Suppl., 58: 81–91.

Poesen, J., 1987. The role of slope angle in surface seal formation. In: V. Gardiner (Editor), International Geomorphology, Proc. Int. Conf. on Geomorphology, Part II. Wiley, Chichester, UK, pp. 437–448.

Proffitt, A.P.B. and Rose, C.W., 1991. Soil erosion processes. I. The relative importance of rainfall detachment and runoff entrainment. Aust. J. Soil Res., 29: 671–683.

Reid, I. and Frostick, L.E., 1987. Toward a better understanding of bedload transport. SEPM Special Publ. No. 39, Tulsa, Oklahoma, pp. 13–19.

Remley, P.A. and Bradford, J.M., 1989. Relationship of soil crust morphology inter-rill erosion parameters. Soil Sci. Soc. Am. J., 53: 1215–1221.

Schultz, J.P., Jarrett, A.R. and Hoover, J.R., 1985. Detachment and splash of a cohesive soil by rainfall. Trans. Am. Soc. Agric. Eng., 28: 1878–1884.

Sharma, M.L. and Uehara, G., 1969. Influence of soil structure on water relations in low humic Latosols: I. Water retention. Soil Sci. Soc. Am. Proc., 32: 765–770.

Sharma, P.P. and Gupta, S.C., 1989. Sand detachment by single raindrops of varying kinetic energy and momentum. Soil Sci. Soc. Am. J., 53: 1005–1010.

Slattery, M.C. and Bryan, R.B., 1992. Laboratory experiments on surface seal development and its effect on interrill erosion processes. J. Soil Sci., 43: 517–529.

Thorne, M.D., 1949. Moisture characteristics of some Hawaiian soils. Soil Sci. Soc. Am. Proc., 14: 38–41.

Torri, D., Sfalanga, M. and Del Sette, M., 1987. Splash detachment: Runoff depth and soil cohesion. Catena, 14: 149–155.

Truman, C.C. and Bradford, J.M., 1990. Effect of antecedent soil moisture on splash detachment under simulated rainfall. Soil Sci., 150: 787–798.

Wicks, J.M., Bathurst, J.C. and Johnson, C.W., 1992. Calibrating SHE soil-erosion model for different land covers. J. Irrig. Drain. Eng., 118: 708–723.

Yang, X. and Madden, L.V., 1993. Effect of ground cover, rain intensity and strawberry plants on splash of simulated raindrops. Agric. Forest Meteorol., 65: 1–20.